Diagenetic processes in the Cueva Formation at El Ribero sector, Burgos (Upper Cretaceous, Basque-Cantabrian Basin, Northern Spain)

Procesos diagenéticos en la Formación de Cueva en el sector de El Ribero, Burgos (Cretácico Superior, Cuenca Vasco-Cantábrica, Norte de España)

M. Erkiaga, F. García-Garmilla, A. Aranburu and J. Elorza

Departamento de Mineralogía y Petrología, Facultad de Ciencias, Universidad del País Vasco, Apdo. 644; 48080 - Bilbao, Vizcaya (Spain)

RESUMEN

En los depósitos carbonatados del Turoniense sup. - Coniaciense inf. de la zona de El Ribero se han reconocido tres procesos diagenéticos principales: silicificación, dolomitización y calcitización. El primero ocurrió en las fases más tempranas de la diagénesis y se tradujo en la formación de nódulos de chert, geodas de cuarzo por reemplazamiento de nódulos de anhidrita, así como el reemplazamiento parcial de diversos fósiles (corales, equinodermos y ostreidos). El segundo proceso diagenético fue una dolomitización intensa pero restringida a las cercanías del actual afloramiento del diapiro de Rosío. Se reconocen en ella dos fases: la primera en cristalitos sucios ricos en inclusiones y la segunda en crecimientos sintaxiales más limpiosque se desarrollan sobre los primeros. Los valores isotópicos de la primera fase $\delta^{18}O$= -2.8‰PDB y $\delta^{13}C$ = 2.3‰PDB) *apoyan un origen marino, en tanto que la dolomita sintaxial (* $\delta^{18}O$= -4.1‰PDB y $\delta^{13}C$ = -0.1‰PDB) *pudo provenir de una zona de mezcla de aguas provocada por el ascenso diapírico sinsedimentario. El último proceso diagenético fue una amplia calcitización relacionada con el límite secuencial de primer orden de 88.5 m.a. Los rombos previos de dolomita fueron dedolomitizados y/o disueltos. Esta fase tambien se manifiesta como un cemento de calcita poikilotópica, cuyos valores isotópicos (* $\delta^{18}O$ = -6.5‰PDB y $\delta^{13}C$ = -8.8‰PDB) *hacen pensar en un origen meteórico.*

Key words: *Upper Cretaceous, Basque-Cantabrian Basin, silicification, dolomitization, calcitization, synsedimentary diapiric activity.*

Geogaceta, 19 (1996), 117-120
ISSN: 0213683X

Introduction and methodology

The Cueva Formation (50-80 m, upper Turonian - lower Coniacian) corresponds to a widespread carbonate ramp that developed in the nord-Castilian platform domain (Floquet, 1991, Fig.1). Considerations about sedimentology and sequential analysis have been made in Erkiaga *et al.* (this volume). A hundred and five rock samples have been collected from mainly carbonate rocks and subjected to the following analyses: a) transmitted light microscopy (using conventional staining techniques); b) cathodoluminescence (CL, accelerating potential of 15 kV at 0.5-0.6 mA beam current and a focused beam diameter of 5 mm); and c) stable isotopes 18O/16O and 13C/12C of calcite and dolomite - the standard procedures of Craig (1957) were employed.

Petrography

Whereas limestone appears as a well-lithified rock, dolomite has a sucrosic texture. Chert nodules are very hard and compact, but when affected by dolomitization, they become pulverized. The original limestone reflects a very shallow marine environment and largely consists of packstone/grainstone microfacies, bearing miliolids, textularids, lituolids, echinoderms, mollusks, bored red algae and even vertebrate remains (Fig.2A). The most common cements are blocky calcite and calcite rims upon echinoderm fragments.

Siliceous nodules and silicified organisms together with cauliflower-type geodes (Chowns and Elkins, 1974) are the most common siliceous manifestations. Microscopic analysis revealed that the silica is biogenic in origin since there are siliceous sponge spicules (Fig.2B) preserved within chert nodules. The quartz of cauliflower geodes very frequently include minute anhydrite laths that mark the growth bands of the crystal (Fig.2C). Silicification contributed to protect fossils and evaporite nodules from further dissolution related to carbonate diagenesis (Elorza and García-Garmilla, 1993).

Dolomite microfacies show crystals about 0.15 mm in size. They are clearly equigranular, have a dirty nucleous and frequently show zoned crystals in which limpid dolomite and pink-stained calcite alternate (Fig.2D). Non-calcitized dolomite facies appear as obscure small rhomb mosaics, whose periphery is coated by limpid dolomite rims (Fig.2E). Under CL, dolomite rhombs show a moderate reddish color, whereas calcite bands are non

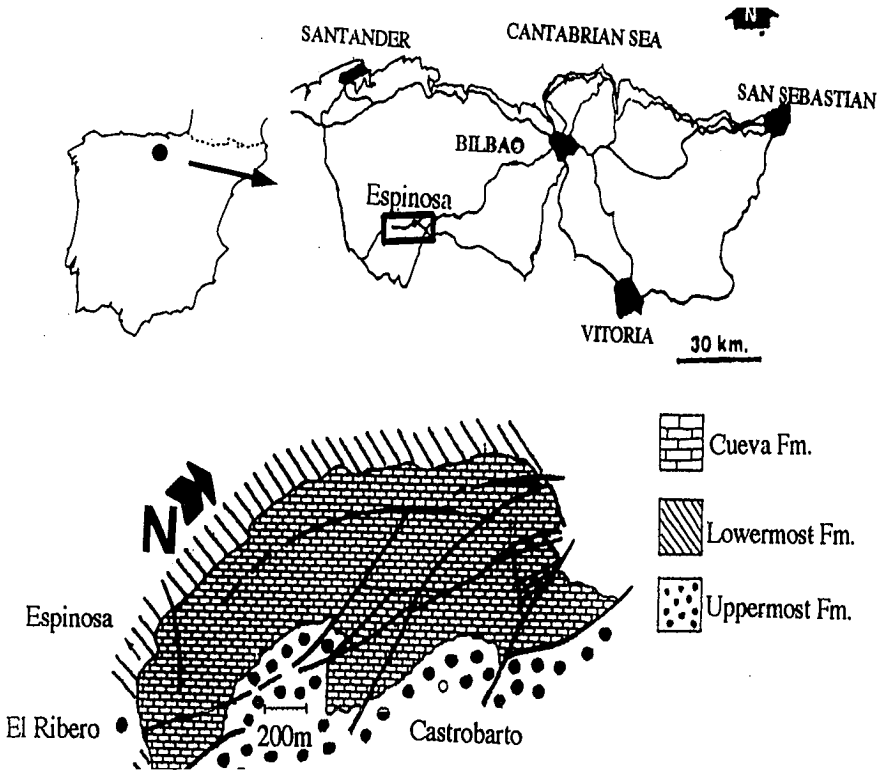

Fig.1.- Geographic and geologic location of the Cueva Formation at El Ribero sector (Northern region of the Burgos province)

Fig.1-Localización geográfica y geológica de la Formación de Cueva en el sector de El Ribero (norte de la provincia de Burgos)

luminescent (Fig.2F).

In addition to radiaxial calcite nodules up to 15 cm in diameter, calcite under the microscope appears as blocky and poikilotopic cements or bands alternating with dolomite in rhombic crystals. Calcite bands of zoned crystals are in optical continuity with the background poikilotopic calcite. Calcite cement was highly destructive in places, corroding dolomite rhombs and leaving isolated rhomb faces included in large calcitic crystals (Fig.2G). Calcite cement which appears infilling the interior of cauliflower quartz geodes, is indicative of a late diagenetic phase. Remobilization of calcite along veins and fractures which occurred much later originated a dedolomitization, which progressively extinguished from the vein to the dolomitized host rock (Fig.2H).

Isotopic results

Fifty two C and O isotopic analyses are plotted in Fig.3. Three families of points can be recognized. Family A corresponds to original limestones; family B to dolomite and family C to calcite infilling pores and paleokarstic cavities.

Conclusions about diagenetic history

Silicification seems to have been an early diagenetic process. Early silicification is inferred from the fact that chert nodules include ghosts of uncompacted primary grains, whereas the carbonate host rock shows compaction and dissolution textures.

Mixing water dolomitization has at present supporters and detractors. On the one hand, Humphrey and Quinn (1989) propose that the abandonment of the mixing zone model is premature, but on the other hand, Whitaker *et al.* (1994) have largely questioned this model. Dolomitization in the El Ribero area affected tens of meters of deposits, and generally occurred downwards. The downward migration of dolomitizing fluids can be inferred from the upper surface of the dolomitized mass, coinciding with the Coniacian Sequence Boundary (CSB) of 88.5 my, whereas the lower surface of the dolomite body is irregular. A lateral migration of dolomitic fluids along bedding planes can also be detected. Dolomitization may have developed over a long time, thus favouring a continuous meteoric water input which travelled across highly porous and permeable sediments. These features suggest a dolomitization process mainly related to a first-order sequence boundary, with synsedimentary diapirism playing a significant role.

The El Ribero dolomite may have resulted from combined dolomitization effects, such as reflux mechanisms derived from marine evaporative lagoonal environments, followed by mixing of marine and meteoric groundwaters. This situation most likely corresponds to a schizohaline diagenetic environment. On the one hand, hypersalinity conditions are represented by small quartz geodes including megaquartz with relict anhydrite laths. On the other hand, the euhedral limpid dolomite crystals, the coarse poikilotopic calcite (which sometimes appears as nodular shapes with radiaxial fibrous crystals), and the zoned dolomite are thought to have originated under a hyposaline regime. Several details of palaeoclimatology in this region during the upper Cretaceous support this possibility, particularly if we take into consideration that the climate was predominantly warm and humid (Floquet, 1991).

Isotopic data from the El Ribero dolomite reflect moderately depleted values and slighty positive C values (Fig.3, family B) similar to those obtained in dolomites which have been interpreted as having a mixed freshwater and seawater origin (Coniglio *et al.*, 1988). These values are also consistent with those of Mutti and Simó (1994) for the Yates Formation (Guadalupian, Capitan Reef Complex), who suggest dolomitization from evaporation-concentrated sea water in slighty reducing conditions. The positive covariance between and C compositions for the El Ribero dolomite suggests a mixing of fresh and sea water as a viable mechanism of dolomitization.

The widespread precipitation of blocky and poikilotopic calcite was the last diagenetic process that affected the rocks at El Ribero. The low C values of equant and poikilotopic calcite (Fig.3, family C), having a cationic content atypical for burial dolomite, suggest carbonates associated with the bacterial sulphate reduction of organic matter (Sass *et al.*, 1991). Nevertheless, the radiaxial calcite has more negative and $\delta^{13}C$ values than other radiaxial fibrous calcites in a subunconformity position, such as those described by Mazzullo *et al.* (1990) in the upper

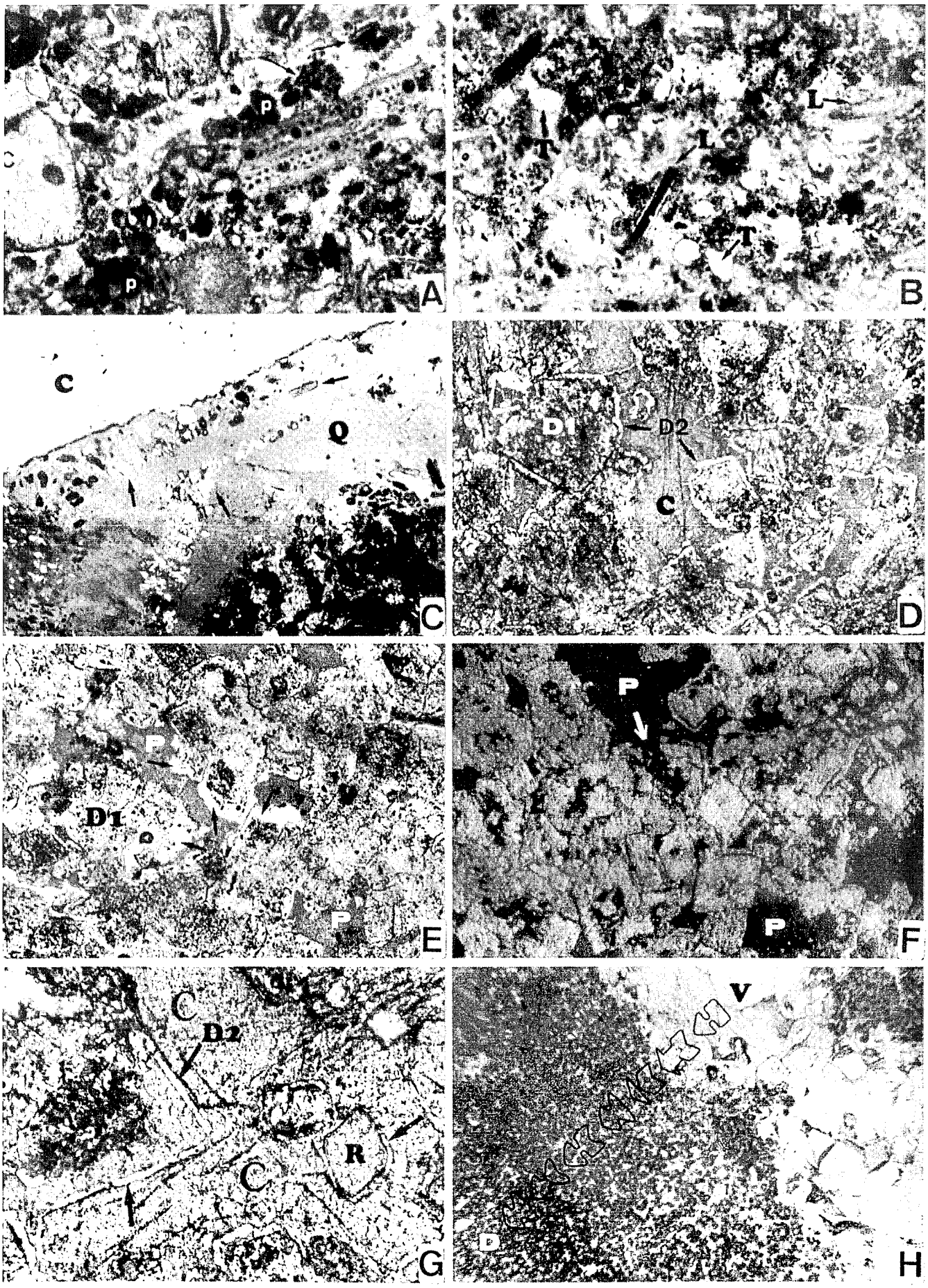
P
P
A
L
T
L
T
B
C
Q
C
D1
D2
C
D
P
D1
P
E
P
P
F
C
D2
C
R
G
V
D
H

Fig.2.- Petrographic images of the Cueva Formation: A) packstone-grainstone host-rock. Peloids (p), cortoids (c), foraminifera (lituolids and miliolids, arrowed) and bone fragments (B). PPL. Photo width 3.25 mm; B) nodular chert including longitudinal (L) and transversal (T) sections of siliceous sponge spicules. PPL. Photo width 2.6 mm; C) cauliflower-type quartz crystal (Q) showing zonations marked by anhydrite laths (arrowed), possible remains of organic matter and dolomite rhombs at the centre. Late poikilotopic calcite (C) completes the pore spaces. XPL. Photo width 1.3 mm; D) composite dirty dolomite crystals (D1) with associated limpid dolomite rims (D2). All are surrounded by later calcite (C). Calcite corroded D1 and selectively replaced between D1 and D2 forming zoned D-C-D crystals. PPL. Photo width 1.3 mm.; E) subhedral D1 crystals coated by later D2 (arrowed) and finally included in poikilotopic calcite (P). PPL. Photo width 1.3 mm.; F) Cathodoluminescence (CL) image showing well-formed dolomite-calcite rhombs. The zonations D1 (reddish) - C (non luminescent) - D2 (reddish) can be distinguished. Later poikilotopic ferroan calcite (P) is associated with dissolution textures (arrowed). Photo width 1.3 mm.; G) calcitization affected mainly D1 crystals. The rims D2 (arrowed) are better preserved from the aggressive precipitation of poikilotopic calcite (C). Dedolomitized D1 rhombs (R) but preserved D2 rims are also observed. PPL. Photo width 0.65 mm.; H) very late remobilization of calcite from a vein (V) and progressive extinguishing of dedolomitization from the vein to the dolomitized host rock (D). Calcitic fluids followed the sense marked by arrows. PPL. Photo width 14 mm.

Fig.2-Petrografía de la Formación de Cueva: A) roca caja (packstone-grainstone). Peloides (p), cortoides (c), foraminíferos (lituólidos y miliólidos, marcados con flechas) y fragmentos óseos (B). Luz transmitida (LT). Anchura de la foto (AF): 3.25 mm; B) nódulo de chert con secciones longitudinales (L) y transversales (T) de espículas de esponjas silíceas. LT. AF: 2.6 mm; C) cristal de cuarzo (Q) de una geoda del tipo «coliflor»; presenta zonaciones marcadas por cristalillos de anhidrita (con flechas), restos de posible materia orgánica y rombos de dolomita en la parte central. La calcita poikilotópica más tardía (C) completa los poros. Luz polarizada (LP). AF: 1.3 mm; D) cristales de dolomita sucia (D1) con crecimientos externos («rims») de dolomita limpia (D2), todos ellos englobados por calcita tardía (C). La calcita corroe los cristales D1 y produce un reemplazamiento selectivo entre D1 y D2 dando lugar a cristales zonados D-C-D. LP. AF: 1.3 mm.; E) cristales subhedrales D1 envueltos por D2 (con flechas) e incluídos en calcita poikilotópica (P). LP. AF: 1.3 mm.; F) imagen de cátodoluminiscencia (CL) que muestra rombos de dolomita-calcita bien formados. Se distinguen zonaciones: D1 (rojiza) - C (no luminiscente) - D2 (rojiza). La calcita férrica poikilotópica (P) está asociada a texturas de disolución (con flechas). AF: 1.3 mm.; G) la calcitización afectó sobre todo a los cristales D1. Los crecimientos D2 (con flechas) están mejor preservados de la precipitación agresiva de calcita poikilotópica (C). Los rombos D1 dedolomitizados (R) conservan los «rims» D2. LP. AF: 0.65 mm.; H) removilización muy tardía de calcita a partir de una vena (V) y amortiguación progresiva de la dedolomitización desde la vena hacia la roca caja dolomítica (D). Las flechas marcan el sentido de migración de los fluídos calcitizantes. LP. AF: 14 mm.

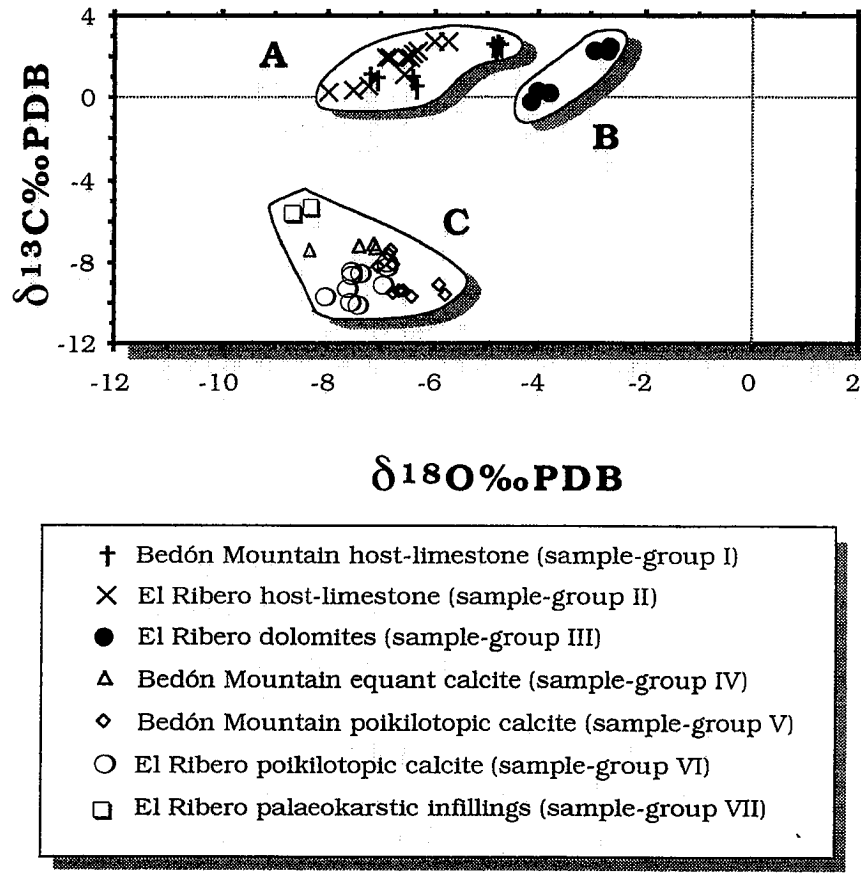

Fig.3.- $\delta^{13}C/\delta^{18}O$ isotopic values for the El Ribero/Bedón Mountain area. The plot shows three families of values(see text).

Fig.3.-Valores isotópicos $\delta^{13}C/\delta^{18}$ para muestras de la zona El Ribero/Bedón. Se distinguen tres familias de puntos: (ver texto).

Triassic of Austria. This leads us to think of a general meteoric freshwater input that did not allow preservation of the possible original marine signal. and $\delta^{13}C$ values for the poikilotopic and blocky calcite at El Ribero are depleted relative to both unaltered dolomite and host limestone (Fig.3, families A and B).

Acknowledgements

This paper has been supported by the Universidad del País Vasco through the Research Project UPV/EHU 130.310-EB059/93. The authors thank David J. Fogarty for correcting the English version of the manuscript.

References

Chowns, T.M. & Elkins, J.E. (1974) *Jour. Sed. Petrol.* 44, 885-903.

Coniglio, M., James, N.P. & Aissaoui, D.M. (1988) *Jour. Sed. Petrol.*, 58, 100-119.

Craig, H. (1957) *Geochim. Cosmochim. Acta.* 12, 133-149.

Elorza, J. & García-Garmilla, F. (1993) *Geol. Mag.* 130, 805-816.

Erkiaga, M., García-Garmilla, F., Aranburu, A. & Elorza, J. (this volume)

Floquet, M. (1991) *Mém Géol. Univ. Dijon.* 14, 1-925.

Humphrey, J.D. & Quinn, T.M. (1989) *Jour. Sedim. Petrol.* 59, 438-454.

Mazzullo, S.J., Bischoff, W.D. & Lobitzer, H. (1990) *Sedimentology* 37,407-425.

Mutti, M. & Simó, T. (1994) Blackwell. *Spec. Publ. Int. Ass. Sediment.* 21, 91-107.

Sass, E., Bein, A. & Almogi-Labin, A. (1991) *Geology.* 19, 839-842.

Whitaker, F.F., Smart, P.L., Vahrenkamp, V.C., Nicholson, H. & Wogelius, R.A. (1994) Blackwell. *Spec. Publ. Int. Ass. Sediment.* 21, 111-132.